Biomaterials 35 (2014) 2420–2427

Contents lists available at ScienceDirect

Biomaterials

journal homepage: www.elsevier.com/locate/biomaterials

Stable corneal regeneration four years after implantation of a cell-free recombinant human collagen scaffold☆, ☆☆

Per Fagerholm [a,1], Neil S. Lagali [a,1], Jeb A. Ong [b], Kimberley Merrett [a,c], W. Bruce Jackson [c], James W. Polarek [d], Erik J. Suuronen [e], Yuwen Liu [f], Isabelle Brunette [b,1], May Griffith [a,d,*,1]

[a] Integrative Regenerative Medicine Centre, Dept. of Clinical and Experimental Medicine, Cell Biology Bldg. – Level 10, Linköping University, SE-581 85 Linköping, Sweden
[b] Department of Ophthalmology, Maisonneuve-Rosemont Hospital, 5415 Boulevard de L'Assomption, Montreal, QC, H1T 2M4, Canada
[c] Ottawa Hospital Research Institute, 501 Smyth Road, Ottawa, Ontario K1H 8L6, Canada
[d] FibroGen, Inc. 409 Illinois Street, San Francisco, CA 94158, USA
[e] Division of Cardiac Surgery, University of Ottawa Heart Institute, 40 Ruskin Street, Ottawa, Ontario K1Y 4W7, Canada
[f] CooperVision Inc., 5870 Stoneridge Drive, Suite 1, Pleasanton, CA 94588, USA

ARTICLE INFO

Article history:
Received 7 November 2013
Accepted 26 November 2013
Available online 25 December 2013

Keywords:
Cornea
Collagen
Transplantation
Recombinant protein

ABSTRACT

We developed cell-free implants, comprising carbodiimide crosslinked recombinant human collagen (RHC), to enable corneal regeneration by endogenous cell recruitment, to address the worldwide shortage of donor corneas. Patients were grafted with RHC implants. Over four years, the regenerated neo-corneas were stably integrated without rejection, without the long immunosuppression regime needed by donor cornea patients. There was no recruitment of inflammatory dendritic cells into the implant area, whereas, even with immunosuppression, donor cornea recipients showed dendritic cell migration into the central cornea and a rejection episode was observed. Regeneration as evidenced by continued nerve and stromal cell repopulation occurred over the four years to approximate the micro-architecture of healthy corneas. Histopathology of a regenerated, clear cornea from a regrafted patient showed normal corneal architecture. Donor human cornea grafted eyes had abnormally tortuous nerves and stromal cell death was found. Implanted patients had a 4-year average corrected visual acuity of 20/54 and gained more than 5 Snellen lines of vision on an eye chart. The visual acuity can be improved with more robust materials for better shape retention. Nevertheless, these RHC implants can achieve stable regeneration and therefore, represent a potentially safe alternative to donor organ transplantation.

1. Introduction

In 2012, the World Health Organization estimated that 285 million people worldwide are visually impaired, while 39 million are blind [1]. Corneal blindness accounts for 5.1% of cases, with 1.5–2 million new cases of unilateral blindness reported annually [2]. While transplantation can cure corneal blindness, there is a severe shortage of donor corneas [2,3]. Although two-year success rates for corneal transplantation are 85% in developed nations like Sweden [4], those for a developing country (e.g. South India) start at 69% [5]. Data from the Australian Corneal Graft Registry shows that the success rate for corneal transplantation is 73% at 5 years and 62% at 10 years [6], which is even lower than for kidney transplantation [7].

As an alternative to donor cornea transplantation, in Fagerholm et al. [8], we showed the regeneration of corneal tissues and nerves after implantation of cell-free, biointeractive corneal implants made from 1-ethyl-3-[3-dimethylaminopropyl]carbodiimide hydrochloride (EDC) and N-hydroxysuccinimide (NHS) crosslinked recombinant human collagen type III (RHCIII). These RHCIII corneal implants were designed as simple mimics of the largely collagenous extracellular matrix of the cornea stroma to stimulate *in situ* regeneration of pathologic corneas.

In the present study, we provide details of the RHCIII implants and report on their four year, long-term progress within the

☆ Four years after grafting of recombinant human collagen-based corneal implants into patients, the overall shape of the patient's regenerated corneas remained stable, while corneal stromal cells and nerves continue to actively regenerate without immunosuppression or immune cell recruitment, confirming the potential of such implants as substitutes for donor human corneas.

* Corresponding author. Integrative Regenerative Medicine Centre, Dept. of Clinical and Experimental Medicine, Cell Biology Bldg. – Level 10, Linköping University, SE-581 85 Linköping, Sweden.
E-mail address: May.Griffith@liu.se (M. Griffith).

[1] Equivalent contributions.

0142-9612/$ – see front matter © 2013 The Authors. Published by Elsevier Ltd. All rights reserved.
http://dx.doi.org/10.1016/j.biomaterials.2013.11.079

corneas of patients. Specifically, we analysed the stability of the regenerated neo-corneas and the time course of the regenerative events. We also compared the immune compatibility of such cell-free, biointeractive implants over four years without immunosuppression against corneas grafted with human donor corneas by penetrating keratoplasty, which is considered the "gold standard" in corneal transplantation [9].

2. Materials and methods

2.1. Biosynthetic corneal implants

Implants were produced under Class 100 conditions in a cleanroom following Good Manufacturing Practice guidelines. Clinical grade recombinant human collagen type III (RHCIII) produced in yeast (*Pichia pastoris*) was purchased from FibroGen, Inc. (San Francisco, CA), dia-filtrated, freeze-dried, and reconstituted to a 10% (w/w) optically clear solution. EDC was supplied by Sigma–Aldrich (St. Louis, MO). NHS was supplied by Fluka (Buchs, Switzerland). Phosphate buffered saline (PBS, pH 7.4) was prepared from the tablet form (Calbiochem Corp., Darmstadt, Germany). Aliquots of 500 μl of RHCIII solution were carefully loaded into a syringe mixing system we previously developed [10], to ensure that the RHCIII solution was free of air bubbles. A predetermined quantity of cross-linker was added based on a molar equivalent ratio of crosslinker: collagen-NH_2 (collagen-NH_2 denotes the ε-amine groups on collagen molecules) of 0.4:1. After thorough mixing at 4 °C, the solution was dispensed into curved polypropylene contact lens moulds (500 μm thick, 10 mm diameter) and cured at 100% humidity at ambient temperature for 24 h. The implants were washed thoroughly in sterile phosphate buffered saline (PBS) and then immersed in PBS containing 1% chloroform to maintain sterility and stored at 4 °C. The EDC and NHS are not incorporated into the final implant [11], circumventing the possibility of toxic breakdown products.

2.2. Characterization of implants

Quality control criteria used to determine release for patient use were visual inspection using a zonometer to ensure smooth, defect-free inner and outer surfaces, and the optical properties of the implant. Briefly, the refractive indices of each fully hydrated implant equilibrated in PBS were measured using an Abbe refractometer (Model C10, VEE GEE Scientific Inc., Kirkland, Washington) at 21 °C with bromonaphthalene as the calibration agent to ensure refractive indices of ≥1.35. A custom-built instrument was used to measure the light transmission of individual samples at room temperature as compared to open beam intensity [12]. The relative percent of light back scattered from the collimated beam by the sample was measured with a circular array of eight photodiodes, 30° off axis. For clinical use, only samples showing light transmission >90% were selected.

Other properties of the implants were also recorded, with all samples tested in triplicate as we previously described [13]. The mechanical properties, tensile strength, moduli and elongation at break, were determined with an Instron mechanical universal tester (Model 3342, Instron, Canton, MA) equipped with a 0.01 kN load cell and Instron Series IX/S software. The crosshead speed was 10 mm min^{-1} and the sampling rate was 10 points s^{-1}. Implants were not pre-stressed. Measurements were taken at room temperature in a >75% humidity chamber.

Thermal stability of PBS-equilibrated hydrogel samples was determined using differential scanning calorimetry (DSC-2C, Perkin Elmer, Waltham, MA; with Thermal Analysis Software system, Instrument Specialists Inc., Spring Grove, IL). Heating scans were recorded in the range of 8–80 °C at a scan rate of 5 °C min^{-1}. PBS equilibrated samples (5–10 mg) were surface-dried with filter paper and then hermetically sealed in aluminium pans to prevent water evaporation. A resulting heat flux vs. temperature curve was then used to calculate the denaturing temperature (T_d) and the enthalpy (ΔH_d). The denaturing temperature is given by the maximum point of the endothermic peak. Enthalpy was determined by integrating the endothermic peak to determine the peak area. The enthalpy of transition, $\Delta H = KA$, where K is the calorimetric constant and A is the area under the curve. The calorimetric constant was pre-determined by the manufacturer.

The water content of PBS-equilibrated hydrogels was measured as follows. Hydrogels were removed from the solution, gently blotted dry with filter paper and immediately weighed on a microbalance to record the wet weight of the sample. Hydrogels of known weight were then dried at room temperature under vacuum to constant weight. The total equilibrated water content of the hydrogels (W_t) was calculated according to the equation:

$$W_t = (W - W_o)/W_w \times 100\%,$$

where W and W_o denote the wet and dry weights of the samples, respectively.

2.3. Clinical study design and treatment

This study was approved by the Linköping Regional Ethical Review Committee and Swedish Medical Products Agency, registered (EudraCT no. 2006-006585-42) and conformed to the Declaration of Helsinki. Subjects were comprised of 10 consecutive patients on the waiting list for corneal transplantation, 8 males and 2 females aged 18–75 years at time of surgery, with keratoconus (9 cases) or central scarring (1 case) [8]. They were grafted with biosynthetic implants by anterior lamellar keratoplasty and retained using overlying sutures, as they were not sufficiently robust for stabilization with running sutures. An additional 9 patients with similar corneal pathologies, 6 males and 3 females aged 40–79 years, with keratoconus (5 cases), endothelial decompensation (2 cases), a deep central scar (1 case) and pseudophakic bullous keratopathy (1 case) were grafted with human donor allograft corneas by full-thickness penetrating keratoplasty, stabilized with peripherally located running sutures. A tenth allografted patient was excluded after a retinal detachment occurred two months postoperatively. Twenty volunteers with healthy corneas, aged 15–88 years, were examined as normal benchmarks.

2.4. Postoperative assessments

Patients were assessed at 1, 3, 6 and 9 months, and 1, 2, 3, and 4 years postoperatively, while healthy volunteers were examined once. Examinations included slit-lamp microscopy, corneal surface sensitivity measurement by Cochet-Bonnet contact esthesiometry, anterior segment optical coherence tomography, and laser-scanning in-vivo confocal microscopy.

2.5. Optical coherence tomography and topographical mapping to measure implant stability

The stability of the implants and regenerated neo-corneas was assessed by examining the changes in thickness and shape over time.

Anterior segment optical coherence tomography was used to monitor the change in corneal thickness. Two-way ANOVA analysis was used with a general linear model to compare central corneal thickness with respect to group and post-operative time. The nonparametric Mann–Whitney Rank Sum test was used where data did not satisfy equal variance testing for the comparison of central corneal thickness at four years in operated groups versus normal healthy corneas. Statistics were performed using statistical software (SigmaStat 3.5 for Windows, Systat Software Inc., Chicago IL).

To map changes in the shape, primarily of the anterior surface over time, corneal topography analyses were performed using a Serial Orbscan II (Bausch and Lomb, Rochester, New York) on all eyes over 4 years. Difference maps and statistics maps were generated according to a protocol we previously developed [14].

2.6. Analysis of antigen presenting dendritic cells as an indication of immune compatibility

In vivo confocal microscope images of the central basal and sub-epithelial areas were analysed to identify the 2 reported morphological types of dendritic cells, the resident antigen presenting cells of the cornea [15]. The 'immature' cells have reflective cell bodies only, while the 'mature' antigen-presenting type have reflective cell bodies bearing one or more short processes termed 'dendrites' [16,17]. In randomized and coded images, the number of each type of dendritic cell per image was manually counted and converted to a density value. Two-way ANOVA analysis was used to compare dendritic cell density with respect to cell subtype and group.

2.7. Histopathology

One patient underwent regrafting since contact lenses required for good visual acuity could not be fitted. A clear corneal button was obtained from this patient and was routinely processed for histopathological examination. Paraffin-embedded sections were stained with haematoxylin and eosin for visualization.

3. Results

3.1. Implants

Properties of the EDC/NHS crosslinked RHCIII implants are shown in Table 1. Optical clarity exceeded that of the average human cornea, which is above 87% transmission [18]. However, the mechanical strength was significantly lower than that of the human cornea [19–21], and implants were much softer, resulting in the need for overlying sutures instead of interrupted sutures for retention. At four years post-operation, examination by slit lamp biomicroscopy showed that the implants were well integrated within the corneas of all 10 patients (Fig. 1).

3.2. Implant stability

Anterior segment optical coherence tomography showed that the shape, thickness, and border areas of engraftment of the implanted corneas remained constant from one to four years post-

Table 1
Properties of EDC/NHS crosslinked recombinant human collagen hydrogels used as corneal implants.

Properties	Transmission (%)	Centre thickness (μm)	Modulus (MPa)	Elongation (%)	Tensile strength (MPa)	Denaturation temperature (°C)	Water content (%)
Implants	95.1 ± 0.05	493 ± 27	1.749 ± 0.782	20.149 ± 7.614	0.286 ± 0.062	54.21 ± 0.91	91.5 ± 0.9
Human cornea	>87	540	3–13		3.81 ± 0.40	65.1	78

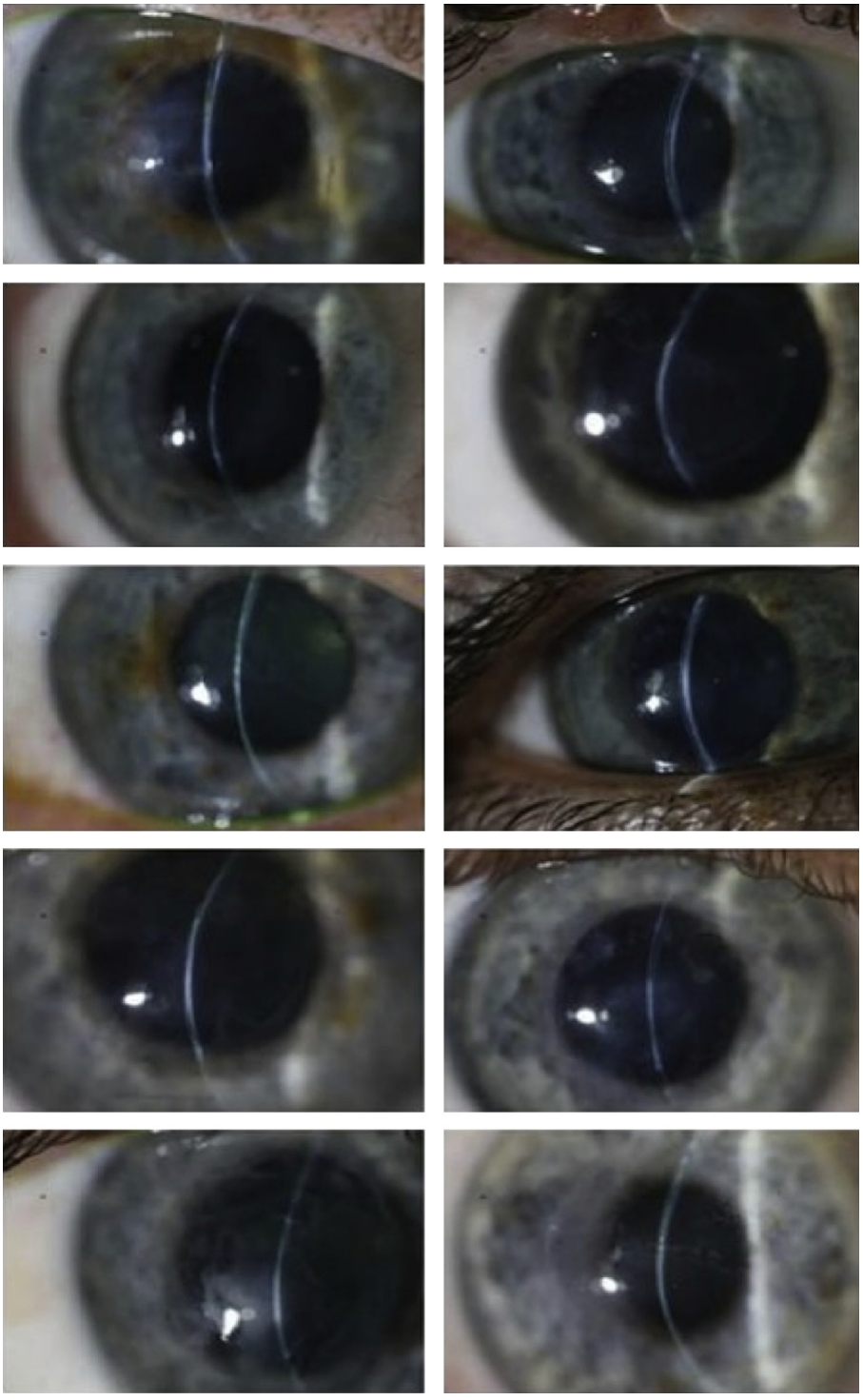

Fig. 1. Slit lamp biomicroscopy images of the corneas of all 10 patients at 4 years after grafting with a biosynthetic implant.

operation (Fig. 2). Beyond an early suture-induced thinning at 3 months post-operation, there was no significant change in corneal thickness from 1 to 4 years postoperatively in either patients with biosynthetic implants or human donor corneas ($p = 0.92$). Central corneal thickness at four years was 358 ± 101 μm in patients with biosynthetic implants, 576 ± 50 μm in patients with human donor corneas, and 534 ± 30 μm in healthy corneas. Biosynthetic corneas were significantly thinner than healthy corneas ($p < 0.001$), while human donor corneas were significantly thicker than healthy corneas ($p = 0.046$).

Detailed 3-dimensional topographical mapping of the nine keratoconus patients' corneas prior to surgery showed the typical pattern of the disease, consisting of a severe paracentral prominence (ectasia) surrounded by a ring of relative depression below the best fit sphere used to describe the shape of the cornea. After surgery, flattening of the cone was sustained to four years in all patients. However, a high degree of surface irregularity was found. This was most likely linked to tight overlying mattress sutures that induced superficial deformation/indentation of the non-rigid implants, as the analyses also confirmed that surface irregularities adopted the hexagonal-shaped paracentral pattern of the tight overlying sutures.

Indeed, apart from focal areas of haze that corresponded to the hexagonal-shaped areas, the rest of the regenerated corneas remained transparent over the four years. In contrast, the donor corneas which received peripherally placed sutures did not show central haze but instead had annular haze at the host–graft interface, which sometimes extended into the grafted area.

3.3. Immune compatibility

In biosynthetic implanted corneas, the sutures were removed at 6.5 weeks (range: 4–7 weeks), after which prophylactic immunosuppressive steroids were stopped. Over the four year post-operative period, no episodes of rejection were observed. The nine patients implanted with donor corneas received steroids for 12 months and sutures were removed after a mean of 13 months (range: 12–18 months). One patient had a rejection episode at one year that resolved after topical dexamethasone treatment.

Large numbers of mature dendritic cells were present in the central region of human donor corneas (Fig. 3B), but not in biosynthetic implants (Fig. 3A) or healthy corneas (Fig. 3C). Mainly immature dendritic cells were observed in both the biosynthetic implants and healthy corneas. The density of dendritic cells (of each type and total) in the patient and healthy volunteer groups at four years is given in Fig. 3D. Total dendritic cell density in the human donor cornea group was significantly greater than in the biosynthetic group ($p = 0.012$). When considering only mature dendritic cells, the density in human donor corneas was significantly increased relative to biosynthetic or healthy corneas ($p < 0.001$), while density in the biosynthetic and healthy groups did not differ ($p > 0.05$).

3.4. Active regeneration of corneal cells and nerves to restore normal morphology

In vivo confocal microscopy showed that the regenerated epithelium remained stratified through the four years post-implantation, with proper density and morphology of the cell layers (Fig. 4A), similar to human donor corneas and healthy controls. At 4 years, the initially cell-free implants were populated by stromal cells that had grown into the implants, but cell-free areas, still remained (Fig. 4A marked with *; Fig. 5). Human donor corneas had fewer stromal cells than healthy corneas, and additionally had small particulate bodies and linear structures indicative of apoptosis, whereas healthy controls had a dense, even distribution of stromal cells. The posterior stromal and endothelial layers, which were untouched during the lamellar surgery, remained healthy and unaffected by the implant at four-years post-operation, as confirmed by histology (Fig. 5).

At 4 years post-operation, the nerves from the plexus lying under the epithelium (subbasal nerves) in the human donor cornea group had reached the central corneal region to varying degrees (Fig. 4A, bottom row). However, they were generally sparse, highly branched and abnormally tortuous. In corneas that received biosynthetic implants, the regenerated nerves followed straighter, parallel paths as described for healthy corneas [22], although the nerve fibres in healthy corneas were thicker and more densely packed.

To test the functional response of the regenerated nerves, central corneal touch sensitivity was assessed by contact esthesiometry in the patients' operated eyes and their contralateral unoperated eyes, which served as controls (Fig. 4B). Two-way ANOVA analysis revealed that touch sensitivity in corneas implanted with human donor and biosynthetic tissue was significantly reduced ($p < 0.001$, both groups) relative to unoperated eyes,

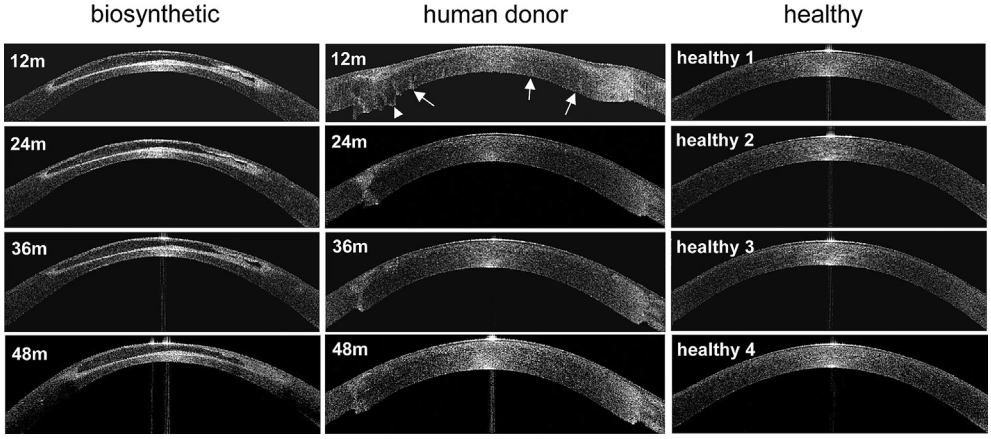

Fig. 2. Anterior segment optical coherence tomography images of the same central cornea, followed over 4 years in biosynthetic and human donor implanted corneas. Left column, biosynthetic implant in a 30 years old female appears stable over time (slight differences are due to slightly different location of sections). Centre column, human donor cornea in a 52 years old male exhibits wound compression due to the sutures, posterior donor-recipient edges mismatch, posterior graft protrusion (arrowhead) and stromal compression lines (arrows) that resolve after suture removal at one year. Right column, appearance of four healthy corneas aged 16–64 years.

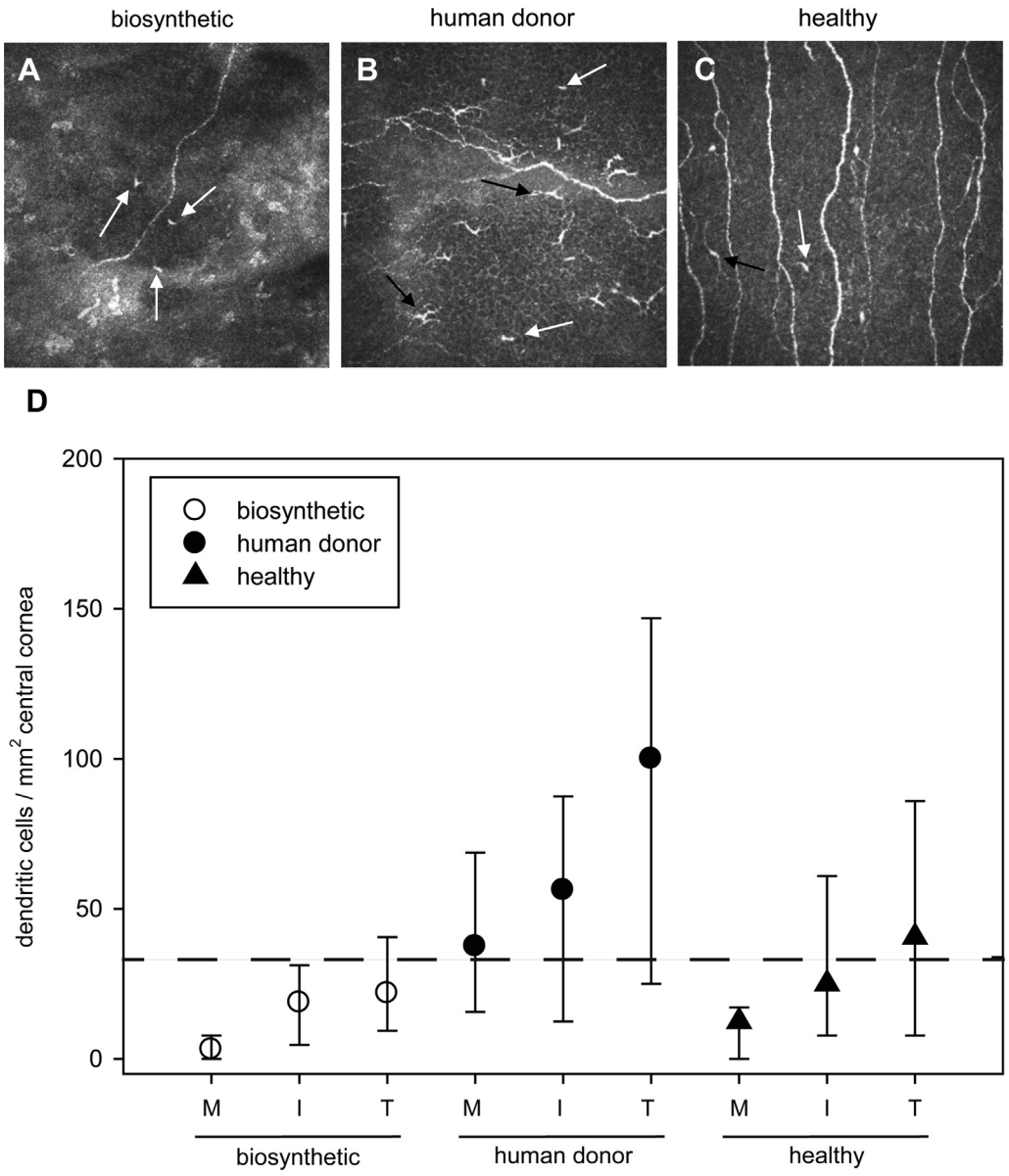

Fig. 3. *In vivo* confocal microscopic images of inflammatory dendritic cells at four years post-operation in regenerated neo-corneas compared to donor cornea grafted and normal, healthy eyes. (A) Few immature dendritic cells (white arrows) are seen in the basal epithelium of a regenerated neo-cornea. (B) Mature (black arrows) and immature (white arrows) dendritic cells in the central basal epithelial region of a cornea grafted with donor tissue, localized to the subbasal nerve plexus. (C) Mature (black arrow) and immature (white arrow) dendritic cells in the normal corneal basal epithelium. Scale bars, 100 μm. (D) Density of dendritic cells in the subbasal epithelium of the central cornea in healthy and 4 year post-operation groups. Data are given as median, 25th and 75th percentiles. M = mature dendritic cells (cell bodies with dendrites), I = immature dendritic cells (cell bodies only), T = total dendritic cells (mature + immature). The dashed line indicates the previously reported mean value of 34 ± 3 cells/mm^2 for the central corneal dendritic cell density in healthy eyes [16].

which consistently exhibited normal touch sensitivity (60 mm). Touch sensitivity in corneas with biosynthetic implants, however, was significantly better than in human donor corneas ($p = 0.04$).

Histology sections through a regenerated neo-cornea showed a normal, healthy corneal architecture, with a stratified non-keratinized epithelium, lamellarly arranged stroma and a layer of endothelium (Fig. 5A). However, there was a cell-free region in the centre of the stroma, which represents the part of the implant that had not yet been remodelled. In areas where the remodelling is more advanced, the implant had blended seamlessly into the stroma (Fig. 5B). The histology, coupled with the in vivo confocal images, supports the contention that active regeneration was still on-going at four years post-operation.

3.5. Corneal visual acuity

Distance-corrected visual acuity was achieved in the biosynthetic group by use of custom-fitted hard contact lenses to regularize an uneven corneal surface, which were tolerated by patients after surgery but not before [8]. In the human donor group, distance-corrected visual acuity was measured with spectacles. At four years, distance-corrected visual acuity was 20/54 and 20/36 in the biosynthetic and human donor groups, respectively. In terms of vision improvement from the preoperative level, the biosynthetic group had a mean gain of 5.6 Snellen lines, while the human donor group had a mean gain of 9.9 Snellen lines at 4 years post-operatively.

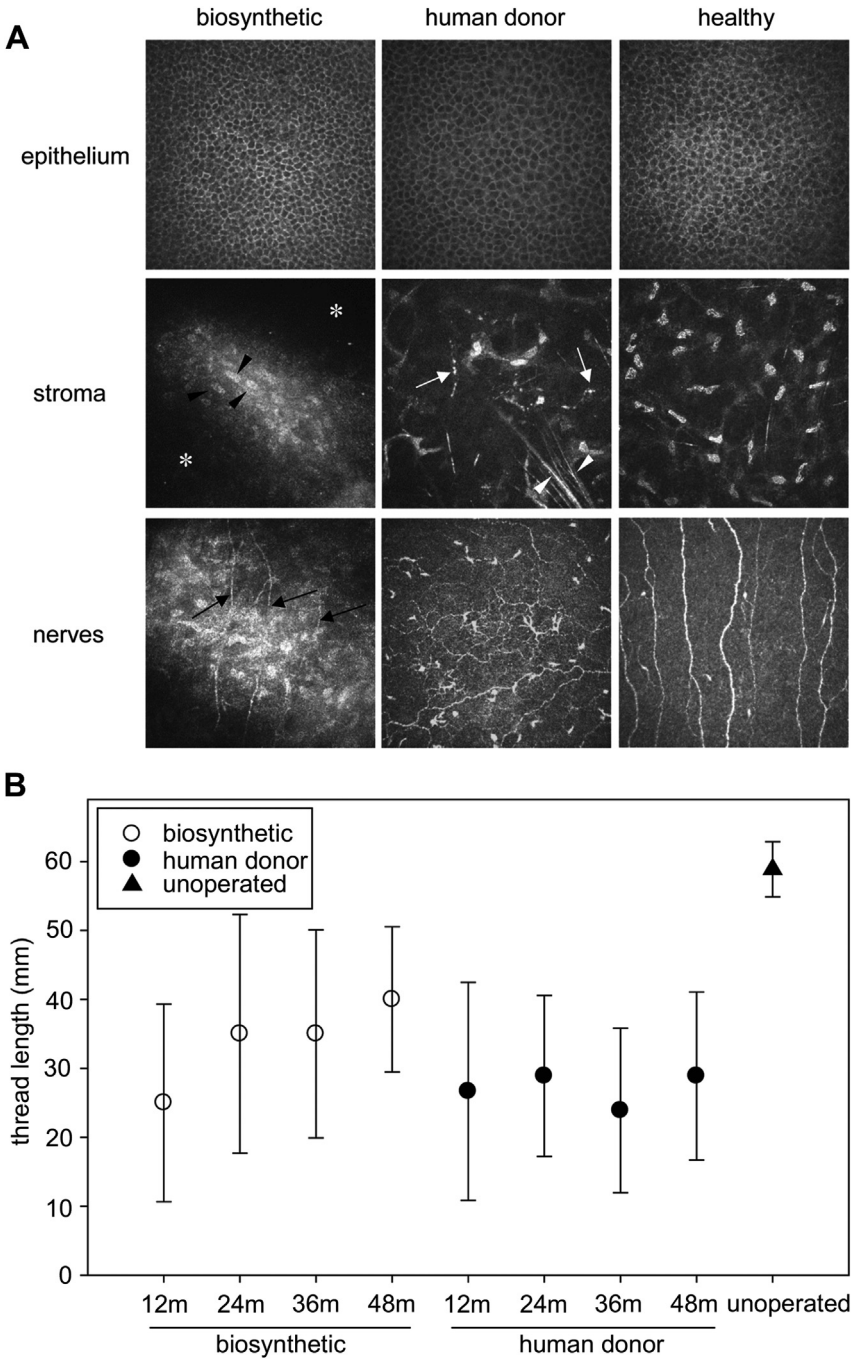

Fig. 4. Typical *in vivo* confocal microscopic appearance of four-year post-operation and unoperated normal corneas (A) and corneal sensitivity to touch measured longitudinally (B). (A) Top row: similar cell morphology is apparent in the regenerated epithelium in operated groups. Middle row: stromal keratocytes (black arrowheads) migrate into the cell-free scaffold (asterisks), while human donor stroma is characterized by fewer keratocytes, linear reflective structures (white arrowheads) and particulate bodies (white arrows) indicative of cell apoptosis. By comparison, the healthy stroma contains a dense, regular distribution of keratocytes. Bottom row: subbasal epithelial nerves in biosynthetic corneas adopted linear, parallel arrangements (black arrows). An absence of Bowman's layer in implants renders keratocytes visible in the same plane as subbasal nerves. In human donor corneas, nerves adopted tortuous paths and dendritic cells were present along with nerves. Dense, parallel nerve architecture is present in the healthy cornea. (B) Epithelial nerve functional testing by esthesiometry indicates hyposensitivity in both operated groups relative to normal corneas, but significantly better sensitivity in biosynthetic implants relative to human donor corneas (two-way ANOVA, $p = 0.04$). Scale bars, 100 μm.

4. Discussion

The biosynthetic implants that we fabricated as grafts were optically transparent but significantly weaker than the human corneas. Nevertheless they were sufficiently robust for grafting. Over four years, these cell-free implants promoted regeneration of corneal tissues and nerves. The regenerated neo-tissues and nerves had stably and seamlessly integrated into the patients' own corneas without requiring immunosuppression beyond a short course of prophylactic steroids. In donor corneal grafts, however, 12 months of immunosuppressive steroids was standard therapy. Even then, one rejection episode out of 9 grafts was observed at one year, corresponding to 11% graft rejection and consistent with the reported rate of 10% within the first two years post-operation in

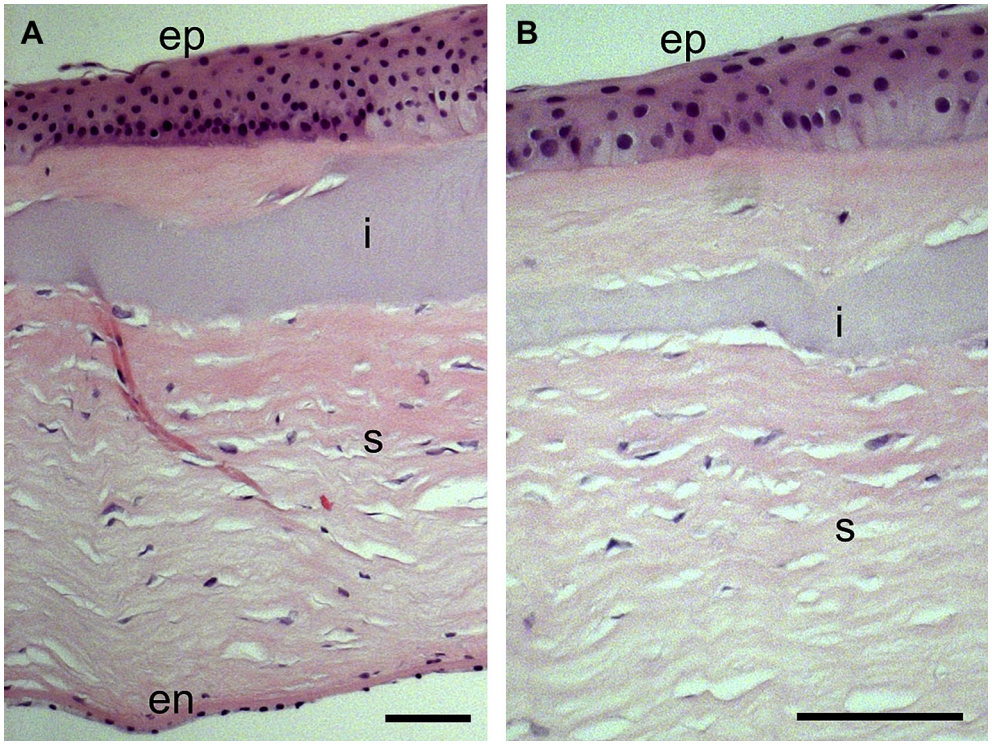

Fig. 5. (A) Haematoxylin–eosin stained histologic section of a regenerated neo-cornea removed after 4 years when the patient was regrafted, showing a normal corneal morphology with stratified epithelium (ep), lamellarly arranged stroma (s) and endothelium (en) that was left intact during the implantation. Part of the recombinant human collagen implant (i) is still present, showing a slow but active remodelling process over time. (B) Higher magnification showing an area of the cornea where remodelling is more advanced and the implant (i) is seamlessly blending into the stroma (s). ep, epithelium. Scale bars, 100 μm.

Sweden [4]. There was no rejection at all in the neo-corneas that had been stimulated to regenerate using cell-free biosynthetic implants. Rejection reactions, although less frequent in lamellar than in penetrating grafts, nevertheless still occur [23,24]. Reports to date imply that the immune reactions in allografts are directed against foreign cells [25,26], suggesting that the cell-free biosynthetic implants may inherently avoid rejection.

At the microscopic level, we found mature antigen presenting dendritic cells in the donor cornea grafted eyes. Dendritic cells serve as immune sentinels, regulating the immunogenicity of the organ, and determine whether a graft is tolerated or rejected [15]. In the healthy cornea, there are very few mature dendritic cells present centrally and immature cells are present in low numbers [16,17]. A proinflammatory environment such as human donor tissue transplantation is needed for their maturation [17,27]. Interestingly, while the donor corneas contained a high density of both immature and mature dendritic cells, only a few, sparsely distributed dendritic cells were observed in the regenerated neo-corneas. Biosynthetic implants, free of foreign-source cells and antigens, appear to avoid dendritic cell activation and/or recruitment, despite the early cessation of topical anti-inflammatory treatment.

Topographical mapping showed that the implants retained their shape over time, indicating stability. The presence of haze, thinning and shape irregularities, however, shows that the overall clinical outcome is dependent upon both the implant properties and the surgical method, i.e. suturing technique used for implantation. Beyond the early thinning caused by the presence of the tight sutures pressing into the implant, there was no change in the thickness or shape of the corneas receiving biosynthetic implants. The use of peripherally located sutures in the human donor implants accounted for the lack of central haze or thinning. A more resilient optical surface that maintains its shape despite suturing would thus be desirable. Hence, we have now significantly increased and reinforced the solids content of our next generation implants and, with it, mechanical strength and the ability to resist suturing-caused surface indentation caused suturing or neovascularization [28].

A functioning stratified epithelium that had regenerated remained stable in the long term in the biosynthetic implants. Corneal nerves are known to serve critical roles in regulation of the tear film and epithelial barrier through the secretion of neurotrophic factors [22]. Here, we show that the subbasal epithelial nerves had re-grown into the central corneal region of biosynthetic implants, and had adopted a regular, parallel-running architecture and have given rise to a blink reflex to touch. The nerve architecture and sensitivity of biosynthetic implants more closely resembled the healthy cornea than human donor tissue. The patients continued to improve in their blink reflex testing sensitivity over the four years.

In vivo confocal microscopy showed that even at four years after implantation, the patients' own stromal cells continued to actively migrate into the initially cell-free biosynthetic implants. Conversely, a sparse stromal cell population and cell death was apparent in human donor tissue. Histology of a regenerated neo-cornea showed a normal corneal morphology with a stratified epithelium and lamellarly arranged stroma, albeit with implant tissue that had not been completely remodelled yet. In summary, the RHCIII implant possesses the ability to guide proper morphological and functional regeneration of corneal tissue.

This study confirms the long-term safety and efficacy for the use of collagen-based biomaterials in regenerating a human tissue. In addition to its use in biosynthetic corneal implants, our work, and that of others, has shown the adaptability and modularity of collagen as a basic building block for multiple tissue types. With adjustments, such as changing the method of fabrication to plastic

compression or electrospinning, or adding other components such as chondroitin sulphate, chitosan, adhesion ligands or growth factors, we have developed regeneration templates for other organ systems [29–32]. A better understanding of the role that the extracellular environment plays in the body's endogenous repair responses will allow for more optimized biomaterial design to meet the requirements for a wide variety of regenerative medicine applications that may soon find their way into the clinic.

5. Conclusion

We have shown that cell-free, biosynthetic implants promoted endogenous regeneration of corneal tissue and nerves that were stable over four years, without any rejection episodes and in the absence of immunosuppression. In terms of aesthetic appearance, resolution of the initial blinding pathology and potential for restoration of vision in the long term, the present study shows that with further development, biosynthetic implants that facilitate endogenous regeneration may be viable long-term options that could one day supplement the supply of human donor tissue for surgical treatment of blinding conditions of the cornea.

Acknowledgements

We thank Monica Söderqvist, for custom hard contact lens fitting for patients at the four-year follow-up. We also thank the Swedish Research Council (PF, MG, NL), County Council of Östergötland, Sweden (PF, MG) and Konung Gustaf V and Drottning Margaretas Frimurarestiftelse, Sweden (PF), and Canadian Institutes of Health Research and FRQS Research in Vision Network, Quebec, Canada (IB) for research support.

References

[1] World Health Organization. Visual impairment and blindness. Fact sheet no. 282. Available from URL:, http://www.who.int/mediacentre/factsheets/fs282/en/index.html; 2012.
[2] World Health Organization. Prevention of blindness and visual impairment: priority eye diseases. Available from URL: http://www.who.int/blindness/causes/priority/en/index9.html.
[3] Cornea transplantation fact sheet. Available from URL: http://www.organdonation.nhs.uk/newsroom/fact_sheets/cornea_transplantation_fact_sheet.asp.
[4] Claesson M, Armitage WJ, Fagerholm P, Stenevi U. Visual outcome in corneal grafts: a preliminary analysis of the Swedish Corneal Transplant Register. Br J Ophthalmol 2002;86:174–80.
[5] Dandona L, Naduvilath TJ, Janarthanan M, Ragu K, Rao GN. Survival analysis and visual outcome in a large series of corneal transplants in India. Br J Ophthalmol 1997;81:726–31.
[6] Williams KA, Lowe MT, Bartlett CM, Kelly L, Coster DJ. The Australian Corneal Graft Registry 2007. Report. Adelaide, Australia: Flinders University Press; 2007. cited in Coster DJ, Jessup CF, Williams KA. Mechanisms of corneal allograft rejection and regional immunosuppression. Eye 2009; 23:1894–7.
[7] Wolfe RA. Long-term renal allograft survival: a cup half-full and half-empty. Am J Transplant 2004;4:1215–6.
[8] Fagerholm P, Lagali NS, Merrett K, Jackson WB, Munger R, Liu Y, et al. A biosynthetic alternative to human donor tissue for inducing corneal regeneration: 24 month follow-up of a phase I clinical study. Sci Transl Med 2010;2:46ra61.
[9] Tan DT. From penetrating to lamellar: the evolution of keratoplasty. Cataract & Refractive Surgery Today Europe. Available from URL:, http://bmctoday.net/crstodayeurope/2013/06/article.asp?f=from-penetrating-to-lamellar-the-evolution-of-keratoplasty; June 2013.
[10] Liu Y, Gan L, Carlsson DJ, Fagerholm P, Lagali N, Watsky MA, et al. A simple, crosslinked collagen tissue substitute for corneal implantation. Invest Ophthalmol Vis Sci 2006;47:1869–75.
[11] Gratzer PF, Lee JM. Control of pH alters the type of cross-linking produced by 1-ethyl-3-(3-dimethylaminopropyl)-carbodiimide (EDC) treatment of acellular matrix vascular grafts. J Biomed Mater Res Appl Biomater 2001;58:172–9.
[12] Priest D, Munger R. A new instrument for monitoring the optical properties of corneas. Invest Ophthalmol Vis Sci 1998;39:S352.
[13] Ahn J-I, Kuffova L, Merrett K, Mitra D, Forrester JV, Li F, et al. Cross-linked collagen hydrogels as corneal implants: effects of sterically bulky versus non-bulky carbodiimides as cross-linkers. Acta Biomater 2013;9:7796–805.
[14] Laliberté JF, Meunier J, Chagnon M, Kieffer JC, Brunette I. Construction of a 3-D atlas of corneal shape. Invest Ophthalmol Vis Sci 2007;48:1072–8.
[15] Mayer WJ, Irschick UM, Moser P, Wurm M, Huemer HP, Romani N, et al. Characterization of antigen-presenting cells in fresh and culture human corneas using novel dendritic cell markers. Invest Ophthalmol Vis Sci 2007;48:4459–67.
[16] Zhivov A, Stave J, Vollmar B, Guthoff R. In vivo confocal microscopic evaluation of Langerhans cell density and distribution in the corneal epithelium of healthy volunteers and contact lens wearers. Cornea 2007;26:47–54.
[17] Mastropasqua L, Nubile M, Lanzini M, Carpineto P, Ciancaglini M, Pannellini T, et al. Epithelial dendritic cell distribution in normal and inflamed human cornea: in vivo confocal microscopy study. Am J Ophthalmol 2006;142:736–44.
[18] Maurice DM. In: Davson H, editor. The eye. New York: Academic Press Inc; 1962. p. 296.
[19] Crabb RA, Chau EP, Evans MC, Barocas VH, Hubel A. Biomechanical and microstructural characteristics of a collagen film-based corneal stroma equivalent. Tissue Eng 2006;12:1565–75.
[20] Jue B, Maurice DM. The mechanical properties of rabbit and human cornea. J Biomech 1986;19:1025–39.
[21] Zeng Y, Yang J, Huang K, Lee Z, Lee X. A comparison of biomechanical properties between human and porcine cornea. J Biomech 2001;34:533–7.
[22] Müller LJ, Marfurt CF, Kruse F, Tervo TM. Corneal nerves: structure, contents and function. Exp Eye Res 2003;76:521–42.
[23] Saini JS, Jain AK, Sukhija J, Saroha V. Indications and outcome of optical partial thickness lamellar keratoplasty. Cornea 2003;22:111–3.
[24] Tan DT, Dart JK, Holland EJ, Kinoshita S. Corneal transplantation. Lancet 2012;379:1749–61.
[25] Koizumi N, Kinoshita S. The surgical treatment for corneal epithelial stem cell deficiency, corneal epithelial defect and peripheral corneal ulcer. In: Dartt DA, Besharse JC, Dana R, editors. Encyclopaedia of the eye, Vol. 4. Italy: Elseiver; 2010. pp. 239–46.
[26] Chong E-M, Dana MR. Graft failure IV. Immunologic mechanisms of corneal transplant rejection. Int Ophthalmol 2008;28:209–22.
[27] Hamrah P, Zhang Q, Liu Y, Dana MR. Novel characterization of MHC class II-negative population of resident corneal Langerhans cell-type dendritic cells. Invest Ophthalmol Vis Sci 2002;43:639–46.
[28] Hackett JM, Lagali N, Merrett K, Edelhauser E, Sun Y, Gan L, et al. Biosynthetic corneal implants for replacement of pathologic corneal tissue: performance in a controlled rabbit alkali burn model. Invest Ophthalmol Vis Sci 2011;52:651–7.
[29] Kuraitis D, Arzhangi Z, Hyatt A, Vulesevica B, Merrett K, Zhang J, et al. Tertiary biomaterial encapsulation controls the release of FGF-2 without impacting bioactivity. Open Tissue Eng Regen Med J 2012;5:43–9.
[30] Kuraitis D, Ebadi D, Zhang P, Rizzuto E, Vulesevic B, Padavan DT, et al. Injected matrix stimulates myogenesis and regeneration of mouse skeletal muscle after ischaemic injury. Eur Cell Mater 2012;24:175–96.
[31] Kuraitis D, Zhang P, Zhang Y, Padavan DT, McEwan K, Sofrenovic T, et al. A stromal cell-derived factor-1 releasing matrix enhances the progenitor cell response and blood vessel growth in ischaemic skeletal muscle. Eur Cell Mater 2011;22:109–23.
[32] Deng C, Zhang P, Vulesevic B, Kuraitis D, Li F, Yang AF, et al. A collagen–chitosan hydrogel for endothelial differentiation and angiogenesis. Tissue Eng Part A 2010;16:3099–109.